ARTICLE IN PRESS

Marine and Petroleum Geology xxx (2008) 1–8

Contents lists available at ScienceDirect

Marine and Petroleum Geology

journal homepage: www.elsevier.com/locate/marpetgeo

Pockmark-like depressions near the Goliat hydrocarbon field, Barents Sea: Morphology and genesis

S. Chand*, L. Rise, D. Ottesen, M.F.J. Dolan, V. Bellec, R. Bøe

Geological Survey of Norway, Leiv Eirikssons Vei 39, 7040 Trondheim, Norway

ARTICLE INFO

Article history:
Received 18 March 2008
Accepted 8 September 2008

Keywords:
Pockmark
Seismic
Multibeam
Barents Sea
Seabed sediments
Soft sediments

ABSTRACT

Pockmarks are observed worldwide along the continental margins and are inferred to be indicators of fluid expulsion. In the present study, we have analysed multibeam bathymetry and 2D/3D seismic data from the south-western Barents Sea, in relation to gas hydrate stability field and sediment type, to examine pockmark genesis. Seismic attributes of the sediments at and beneath the seafloor have been analysed to study the factors related to pockmark formation. The seabed depths in the study area are just outside the methane hydrate stability field, but the presence of higher order hydrocarbon gases such as ethane and/or propane in the expelled fluids may cause localised gas hydrate formation. The selective occurrence of pockmarks in regions of specific seabed sediment types indicates that their formation is more closely related to the type of seabed sediment than the source path of fluid venting such as faults. The presence of high acoustic backscatter amplitudes at the centre of the pockmarks indicates harder/coarser sediments, likely linked to removal of soft material. The pockmarks show high seismic reflection amplitudes along their fringes indicating deposition of carbonates precipitated from upwelling fluids. High seismic amplitude gas anomalies underlying the region away from the pockmarks indicate active fluid flow from hydrocarbon source rocks beneath, which is blocked by overlying less permeable formations. In areas of consolidated sediments, the upward flow is limited to open fault locations, while soft sediment areas allow diffused flow of fluids and hence formation of pockmarks over a wider region, through removal of fine-grained material.

1. Introduction

Surface, and near-surface, indications of migrating hydrocarbons provide the petroleum systems analyst critical information about source, maturation and migration (Abrams, 2005). The rate, and volume, of hydrocarbon seepage to the surface greatly controls near-surface geological and biological responses. Analysis of these parameters is therefore the most effective method for detection of hydrocarbon leakage. Often, the escape of such fluids to the water column is coincident with the presence of pockmarks. In this study we attempt to establish the morphology, genesis and various other factors associated with the formation of pockmarks.

Pockmarks are described as circular to oval depressions found on the seafloor (King and MacLean, 1970) and may appear as single features, as groups, or as longer chains (Hovland, 1981). Individual pockmark sizes vary from a few metres (limited by data resolution) to more than 400 m in diameter and 2 to more than 15 m in depth. Elongated pockmarks are observed to have their long axis orientation along the prevailing bottom current direction (Farin, 1980; Bøe et al., 1998). Their genesis can be due to many factors, including expulsion of water by the melting of deeper lying permafrost (Farin, 1980; King, 1980), dissociation of gas hydrates (Mienert et al., 1998), freshwater seepage through artesian aquifers (Whiticar and Werner, 1981) or escape of hydrocarbon fluids from underlying petrogenic source rocks (King and MacLean, 1970; McQuillin et al., 1979; Rise et al., 1999). Some studies suggest that the formation and preservation of pockmarks are closely related to sediment type (e.g., Hovland, 1981). However, it is still not clear whether one can relate pockmark formation to one of these mechanisms alone. Since pockmarks are essentially escape phenomena of gas or fluid from the sediment/bedrock, most often fine-grained sediment will be brought into suspension and transported away by currents. Hence, soft fine-grained sediment is often suggested as a necessary recording medium for the formation of pockmarks.

2. Regional setting

Pockmarks are observed along most of the Norwegian offshore region including the Barents Sea (Solheim and Elverhøi, 1985; Hovland, 1981; Ginsburg et al., 1999), North Sea (Van Weering,

* Corresponding author. Tel.: +47 73904283; fax: +47 73921620.
E-mail address: shyam.chand@ngu.no (S. Chand).

0264-8172/$ – see front matter © 2008 Published by Elsevier Ltd.
doi:10.1016/j.marpetgeo.2008.09.002

1982), Skagerrak (Bøe et al., 1998; Rise et al., 1999) and also along the mid-Norwegian margin (Buenz and Mienert, 2004). Pockmarks from the North Sea have been suggested to have petrogenic origin (Van Weering, 1982; Van Weering et al., 1973; McQuillin et al., 1979; Maisey et al., 1980; Hovland, 1981), even though some studies suggest an artesian ground water flow origin (Hubscher and Borowski, 2006). No pockmarks have been reported south of 56° N in the North Sea, which Hovland (1981) attributed to the seabed sediment type rather than the absence of gas seepages (Hovland, 1983; Hovland and Judd, 1988; Rise et al., 1984).

Pockmarks in gas hydrate provinces are often associated with boundaries of gas hydrate stability (Mienert et al., 1998), however, studies along the mid-Norwegian margin show that the pockmarks can form within the Gas Hydrate Stability Zone (GHSZ) even where a regional Bottom Simulating Reflector (BSR) exists (Hovland et al., 2005; Buenz and Mienert, 2004; Buenz et al., 2005). High-resolution seismic data from this region clearly shows that the near-surface sedimentary bedding is impregnated with vertical pipe structures underlying the pockmarks, and that the pipes are deeply rooted (Buenz and Mienert, 2004; Buenz et al., 2005). Sampling near this area shows that the micro-seepage is still active, and may indicate that the pipes represent fluid flow conduits which transport both bacterial and thermogenic hydrocarbons into the water column (Hovland et al., 2005). Pockmark occurrences can also be related to the hydrocarbon potential of the underlying formation. The Skagerrak region of the North Sea provides the best example for this case where pockmarks are concentrated along outcrops of middle Jurassic sandstones (Rise et al., 1999), even though soft sediments cover larger areas. In light of these complex processes related to pockmarks, we have made a detailed study of a pockmark region using multiple methods.

The present study area falls in the vicinity of the Goliat hydrocarbon field and the Tromsøflaket bank along the south-western part of the Barents Sea (Fig. 1). The region is characterized by an elongate glacial depression, the Ingøydjupet, extending from near shore to the Bear Island Trough in the north. The whole Barents Sea has been subject to broad scale glacial erosion by which a large amount of sediment was removed. Most of the eroded material was transported along the Bear Island Trough and deposited beyond the shelf edge on the Bear Island Trough mouth fan (Vorren et al., 1991). Most of Tromsøflaket and Ingøydjupet, where Goliat is located, have undergone substantial erosion (Vorren et al., 1991; Hjelstuen et al., 2004). Tromsøflaket comprises till deposits up to 150 m thick and contains hardly any soft sediments. In Ingøydjupet, soft post-glacial sediments, up to 15 m thick, have been deposited over tills overlying the upper regional unconformity (URU) (Vorren et al., 1991). Here, we have looked at various signatures of pockmarks in multibeam bathymetry (MBB) and 2D/3D seismic data (Fig. 1). These data provide insight into the geological processes influencing their formation. This study was done partly for the MAREANO (www.mareano.no) project, which covers the southern Barents Sea.

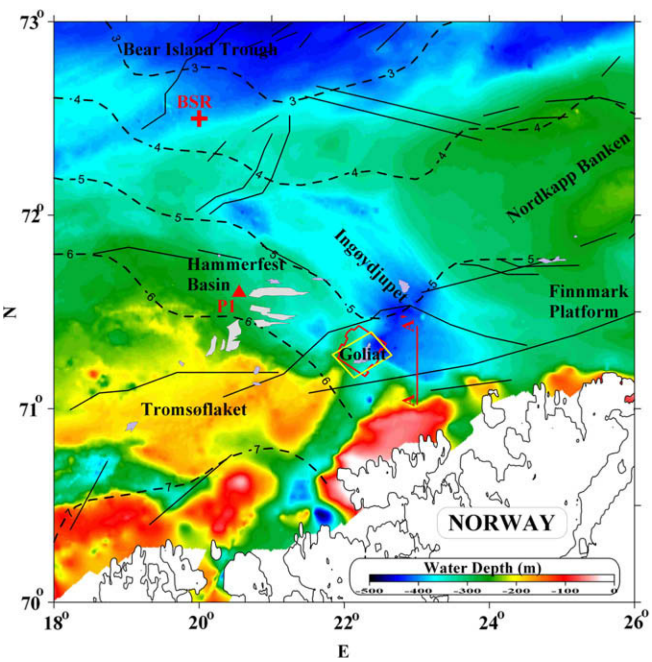

Fig. 1. Bathymetry from the southern Barents Sea showing locations of multibeam bathymetry (yellow rectangle) and 3D seismic surveys (red polygon). Also shown are locations of major faults (black lines), pockmarks from Hovland and Judd (1988) (solid red triangle), BSR (red plus; Andreassen et al., 1990) and major oil/gas discoveries (grey). The dashed contours show the bottom water temperature of the area (WOD05, 2005). 2D seismic line A–A′ from IKU is also shown (red line) (Fig. 8).

3. Methods

In 2005–2006, about 3500 km^2 of multibeam bathymetry and backscatter data were collected from the study area, in water depths of 180–450 m and we used part of this dataset in the present study (Fig. 1). The multibeam data were collected by a Kongsberg Simrad EM1002 (95 kHz) system, designed for seabed mapping in continental shelf depths ($\sim$10–1000 m). Data density in the study area was suitable for the production of raster grids, of both bathymetry and backscatter data, at 10 m resolution (cell size), which provides sufficient detail for the discrimination of pockmarks. While the bathymetry provides a good indication of the location and dimensions of pockmarks, the co-registered backscatter data provide information on the nature of the surficial sediments. The amplitude of the return from the seabed, once ground-truthed with samples or observations, can provide a proxy to sediment grain size distribution (e.g., Todd et al., 1999). Bellec et al. (2008) used box core, van Veen grab, multi-core samples, and video inspection to characterise the sediments in the study area.

The conventional 3D seismic data acquired by ENI Norge for deeper hydrocarbon exploration of the Goliat Field was also available for our study. The data were processed to create an equally spaced grid (12.5 m). Data were migrated to remove artefacts formed in the subsurface seismic data due to presence of curved features such as synclines/anticlines and sharp features such as faults. The final migrated data was then interpreted using Geographics Seisvision software to derive the bathymetry and other attributes such as frequency, reflection strength, etc. The total amplitude reflection strength of the first half cycle is derived by calculating the amplitude of the seismic pulse between the seafloor reflection (zero amplitude) and half wavelength below it (5 ms). The peak wavelength of the seismic data is around 100 Hz and hence the wavelength is 16 m (using 1600 m/s velocity). This attribute will give constructive and destructive interference effects of the seismic signal at boundaries where two reflectors are discordant. The absolute amplitude of the seismic section for a particular two-way time (TWT) interval is also calculated by adding the instantaneous unsigned normalized amplitudes of the seismic trace between the seafloor reflector and the TWT of interest. This attribute will highlight anomalous amplitudes within the depth interval of interest. An analogue 2D near trace seismic record from mini-airgun is used for regional analysis of the area.

4. Interpretation of multibeam bathymetry and 2D/3D seismic data

The high-resolution (10 m cell size) MBB image reveals the detailed morphology of the seafloor (Fig. 2). We observe that

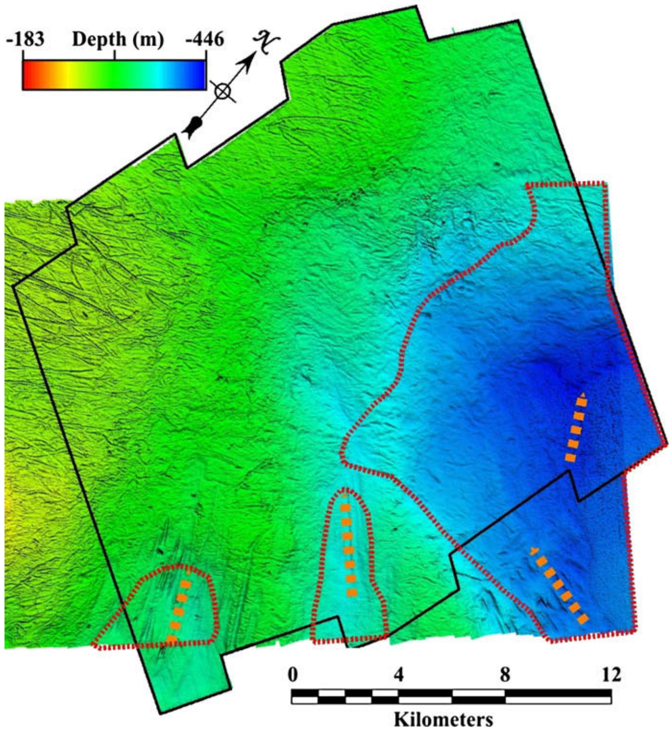

Fig. 2. Shaded relief bathymetry from multibeam bathymetric (MBB) survey and 3D seismic (region outside MBB). Notice the lineations formed by ice sheet movement during the last glacial maximum (orange arrows). Pockmarks (red polygons) are located in depressions with fine-grained sediments and mainly concentrated in the depression shown at right side of the figure. The location of the 3D seismic block (black polygon) and the study area is shown in Fig. 1.

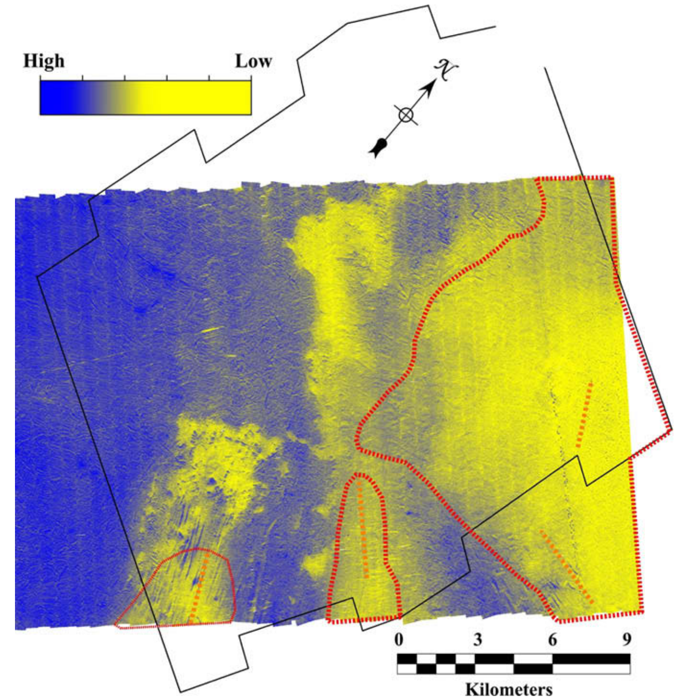

Fig. 3. Backscatter map from the study area showing the variation in backscatter depending mainly on seabed sediment type. The pockmark regions shown with dotted polygons give slightly lower amplitudes compared to other regions, while the pockmarks can be seen with high backscatter values. Notice the presence of low backscatter values outside the pockmark region along the top centre of the figure, indicating a similar medium to that in pockmark region.

pockmarks are concentrated along some local depressions. Iceberg ploughmarks and glacial lineations can clearly be seen in the shallower areas and the platform-like area along the SW side of the survey region. Iceberg ploughmarks are very common. Glacial lineations, formed by scouring glaciers, can be seen as channels along the southern part of the survey area, and some of them coincide with pockmark locations. The pockmarks have diameters generally less than 50 m. They are concentrated in Ingøydjupet, where up to 15 m of fine-grained sediments occur at the seabed (Svitzer, 2001). The sediment thickness decreases towards the peripheries of the basin, where it is less than a metre, so also the depths and sizes of the pockmarks. Hence, the two sub-regions with glacial lineations (Fig. 2), and the outer parts of the major pockmark area with a thin veneer of sediments, have pockmarks that are smaller than in the deepest part of the main pockmark area. The pockmarks in the deepest part of Ingøydjupet are up to 100 m in diameter and 10 m deep. Pockmarks in the peripheries of the depression, and also in the small depressions, have diameters from 35 to 45 m and depths from 1 to 2 m. The density of pockmarks also decreases from 210 to 135/km^2 as we move away from the deepest part of the basin.

Most of the areas outside these depressions are devoid of pockmarks. Some large pockmark-like depressions were probably formed by icebergs impinging the seafloor (e.g., Bass and Woodworth-Lynas, 1988; Eden and Eyles, 2001). The multibeam backscatter image of the seafloor suggests correlation between sediment type and reflectivity (Figs. 3 and 4). Pockmarks are located in soft sediment areas with low backscatter compared to the poorly sorted till deposits, comprising a thin surficial layer of sand and gravel, along the bathymetric highs (Bellec et al., 2008) (Fig. 4). Photographs taken outside pockmarks show muddy seafloor with a large number of furrows. A detailed description of the sediment character and its relation to the backscatter are discussed by Bellec et al. (2008) and are not considered further here.

Bathymetry derived from 3D seismic is also shown outside the MBB data since they have lower resolution due to a line spacing of 12.5 m (Fig. 1). However, the spatial resolution of the data is good enough to see pockmark-like depressions in the same areas as observed on the MBB data set (Fig. 2). The main difference between the two bathymetries is that smaller pockmarks along the basin peripheries are invisible due to the lower spatial resolution of the 3D seismic data. However, the 3D seismic data have the advantage that collective attribute information can be deduced on the subsurface sediment properties. We can not only extract the seabed reflectivity, but also other parameters such as frequency, phase angle, sub-seabed reflectivity, etc. which give additional information regarding the attenuative and other properties of the medium. The seabed reflector amplitude from the 3D seismic represents the composite amplitude response of the top 8 m depth below seafloor since the wavelength of the seismic signal is around 16 m (peak frequency 100 Hz). The total amplitude map of the first half cycle of the seismic trace shows a clear variation, which may be related to the thin veneer of surface sediments and discordant layers underneath (Fig. 5). The discordant reflections are due to 'tuning' of the seismic signal by constructive and destructive interferences from layers abutting the seafloor (Widess, 1973). In the soft sediment region along the SE corner of the study area, clear variation in seabed character can be seen associated with pockmarks, similar to those observed in the backscatter image (Fig. 3). This region is also characterized by a drop in frequency content again due to the highly attenuative nature of the soft sediments.

A closer inspection of the area with high pockmark concentration using MBB, backscatter and seismic attributes brings out some

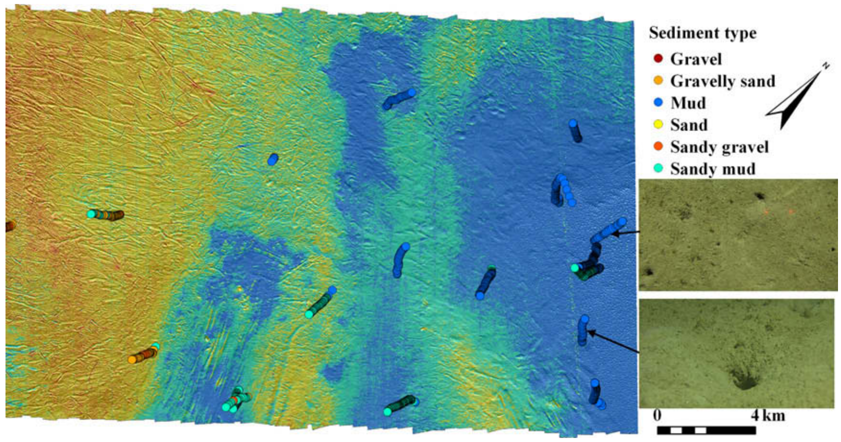

Fig. 4. Backscatter classified in sediment classes (see legend) according to the ground-truthing (video lines and samples). Interpreted video transects are plotted on the backscatter. The two video pictures display muddy sediments, 10 cm between the red spots. Notice the region with mud devoid of pockmarks along the top centre as shown in Fig. 3.

interesting observations (Fig. 6). At many pockmarks, there is an increase in backscatter values (Fig. 6b and d). Also, the seismic reflection amplitude shows an increase in value coincident with pockmark locations (Fig. 6f). In fact, the rims of the pockmarks show higher seismic reflection amplitude compared to both the region inside and outside the pockmarks (Fig. 6f). Since the seismic reflection represents a composite thickness of a few metres below the seafloor, the increase in amplitude towards the rim can possibly be attributed to deposition of carbonate material along the side-walls of the pockmark. This is slightly different from the back-scatter, where we can clearly see the changes in sediment character. Since the frequency used for seismic data acquisition is quite low (100 Hz), the nature of the reflection is also different. Here the rigidity of a few metres of sediment is seen rather than a few tens of centimetres in the case of MBB. Hence loose sandy sediments towards the centre of the pockmark give a signature almost similar to that of loose fine-grained sediments outside pockmarks, in the seismic data. We also notice that pockmark concentration is higher along a NW–SE trending linear feature (Fig. 6c and e), which is suspected to be a relict feature from a deep scouring iceberg ploughmark.

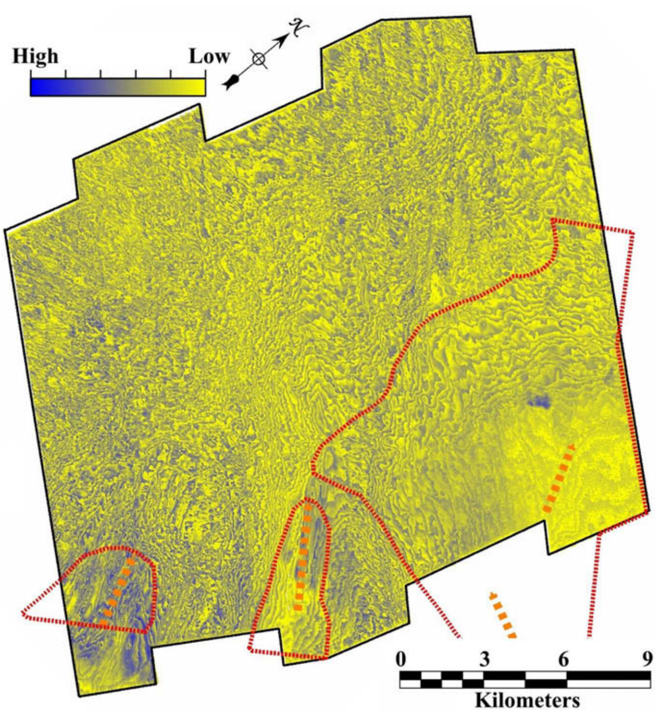

Fig. 5. Total amplitude reflection map of the first half cycle of the seabed reflection from 3D seismic data. Notice the bands of changes in amplitude towards the depo-centre of fine-grained post-glacial sediments at the NE corner. The depo-centre is showing low amplitudes, denoting high energy loss due to the presence of a 5–10 m thick layer of soft sediments.

The absolute amplitude (unsigned amplitudes) of the seismic reflections from the top 150 ms TWT of the seismic traces below the seafloor shows that the region of pockmarks is essentially very transparent with low reflectivity values (Fig. 7). Patches of high reflectivity can be seen in some areas away from the pockmark region, indicating high reflectivity surfaces underneath the seafloor. Also one can see the indication of a NNE–SSW running fault, F1, which could be acting as a conduit for the passage of gas and other fluids from below (Fig. 7). Fault F2, which is also running in NNE–SSW direction, partially coincides with the muddy, low backscatter region (Figs. 3 and 4), but it is not associated with pockmarks, indicating that it is closed. High-resolution mini-airgun seismic profiles across the area show that the Quaternary sediment thickness increases to as much as 100 ms TWT in the deepest part of Ingøydjupet (Fig. 8, line A–A′). A transparent zone of total blanking can be noticed in the upper few tens of milliseconds, indicating presence of gas in the very loose soft sediments. The sediments below the base Quaternary unconformity were tilted before erosion took place (Fig. 8). A closer look on seismic profiles along the high total reflection amplitude zones in the reflectivity map shows that they are associated with high amplitude reflections from shallow gas reservoir pockets (Fig. 9). The enhanced reflections are mainly concentrated in the region without pockmarks. Acoustic blanking and faults connecting to deeper levels occur beneath these amplitude anomalies, denoting a deeper origin for the gas causing these anomalies, implying a thermogenic fluid escape origin.

5. Discussion

Our interpretation of multibeam bathymetry and near-surface seismic data highlights the indicators of an active hydrocarbon system. Presence of brightened reflectors connected downwards through near vertical faults, and the confinement of such reflections to certain depths invite attention (Figs. 7 and 8). Enhanced amplitudes in seismic reflection sections can be due to higher amounts of gas hydrates, which attenuate seismic amplitudes (Chand and Minshull, 2004), as happens in the presence of

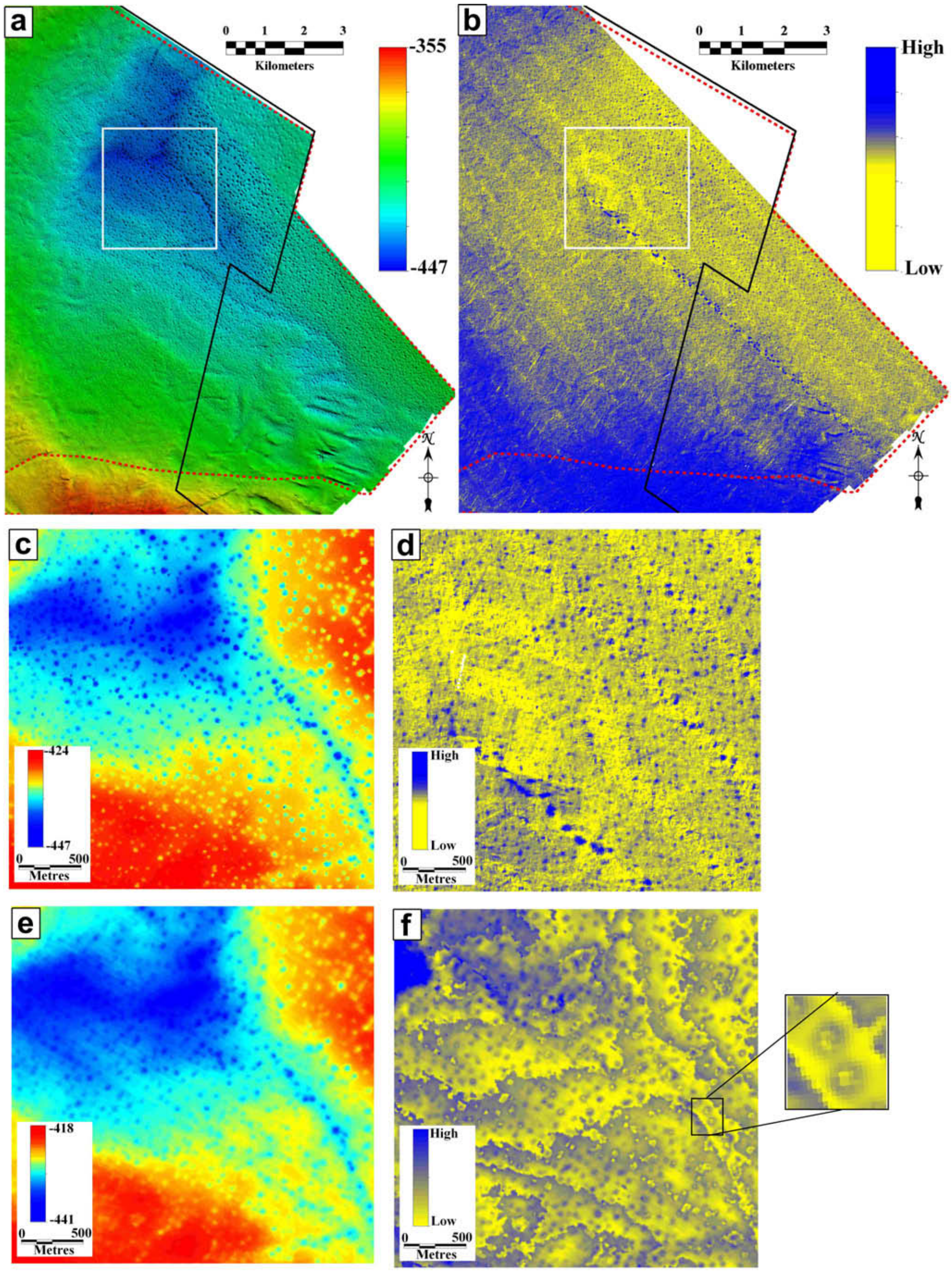

Fig. 6. Pockmark region (a) bathymetry from multibeam and 3D seismic data (region outside MBB data); (b) backscatter from multibeam data, (c) detailed bathymetry showing pockmarks and (d) corresponding backscatter signatures; (e) bathymetry of the same area from 3D seismic and (f) corresponding total amplitude reflection of first half cycle seafloor reflection from 3D seismic. The locations of figures (c) to (f) are shown in figures (a) and (b) (white rectangle). Notice the concentration of pockmarks along semi-filled NW–SE trending iceberg ploughmark along the right side of the figures (c) and (e). The pockmarks are seen with high backscatter values while seismic reflectivity values show elevated values along their rims (see the blow up figure).

gas. Only a small amount of gas is necessary to produce large attenuation of seismic amplitudes and drop in seismic wave velocity, but to produce a similar kind of attenuation and enhanced reflections, a large amount of gas hydrate needs to be present. Since gas hydrates and gas behave similarly regarding attenuation (Guerin and Goldberg, 2002) and enhancement of amplitudes (Bellefleur et al., 2006; Hardage et al., 2006; Nouze et al., 2004), except for the difference in polarity, it is difficult to separate them (unless a proper GHSZ boundary is established). Enhanced reflections are observed in different geological provinces such as Mallik (Bellefleur et al., 2006), Nankai Trough (Nouze et al., 2004) and Gulf of Mexico (Hardage et al., 2006), which we hence attribute to the property of gas hydrate itself.

Often in marine settings where sediments are permeable and porous, continuity in fluid migration results in demarcation of a clear boundary between gas and gas hydrates, which is usually observed as a BSR. In regions where the BSR depths are very large due to large amount of higher order hydrocarbon gases (such as Gulf of Mexico, Sassen et al., 2001), the BSR will be patchy and limited to basin boundaries where it intersects the seafloor. Similar enhanced reflections are seen in regions of gas and gas hydrate

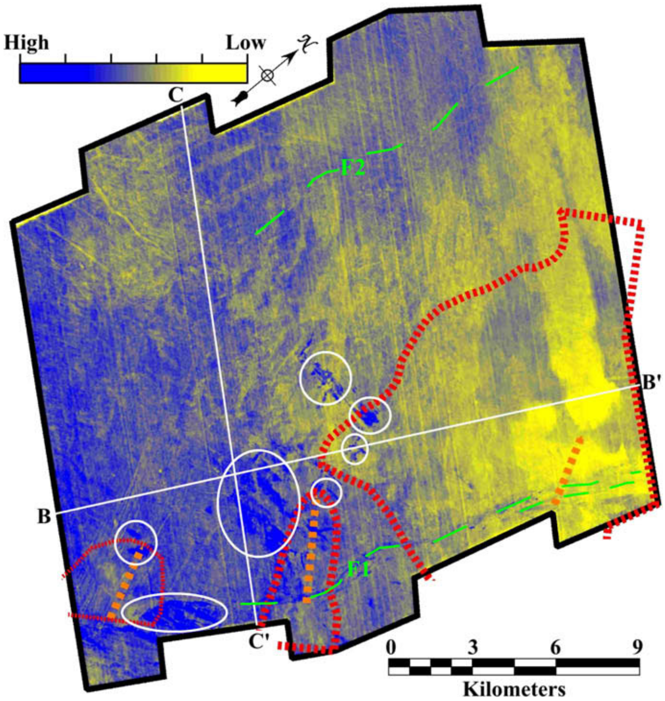

Fig. 7. Average absolute amplitude map of the upper 150 ms below the seafloor. Notice the low amplitudes along the bottom-right corner of the 3D seismic block denoting high attenuation of P-waves due to non-compacted, loose sediments. Gas anomalies can be noticed along the bottom-left region (white circles). They correspond to gas pockets locked up as patches. Two major faults (F1 and F2) running in NNE–SSW direction are also shown (green dashed line). The vertical throw of fault F1 is shown in Fig. 9. The locations of seismic sections shown in Fig. 9 are also shown (white lines).

without the presence of a BSR (e.g., Mallik, Bellefleur et al., 2006) if the gas flow is controlled by formation properties such as porosity and permeability, and faults. Depending on the gas hydrate stability conditions, gas either forms hydrate or, if there are open pathways, the gas escapes into the overlying water column, creating a pockmark if soft sediment is available.

Formation of pockmarks in areas of soft sediments is observed worldwide. In areas where no recording medium is available, pockmarks do not form, and it is difficult to locate fluid venting activity. In such locations, biological activity and carbonate crusts may still be prevalent and a large community may be thriving on it (Macdonald et al., 2003). MBB data can locate such small-scale features on the seafloor (e.g., Paull et al., 2002). Buenz et al. (2005) observed similar anomalies related to pockmarks along the mid-Norwegian margin and are interpreted to have formed from fluid expulsion through polygonal faults connected to deeper reservoirs. Recent studies have shown that the focussed fluid flow in consolidated sediments changes to diffused flow in soft shallow subsurface, leaving out any direct expression to subsurface conduits (Van Rensbergen et al., 2007). Consistent with our observations, it has also been seen elsewhere that deep iceberg ploughmarks act as easy escape routes for the flow of fluids, and thereby creation of pockmarks (Solheim and Elverhøi, 1985; Rise et al., 1999; Van Rensbergen et al., 2007).

Gas/fluid seepages are frequently associated with the occurrence of authigenic carbonate mineralisation because of microbially mediated oxidation of methane (Ritger et al., 1987; Boetius et al., 2000). This is consistent with the observation of high amplitude seabed reflections possibly due to carbonate along peripheries of pockmarks in our seismic data. Also, carbonate reef structures are reported from nearby Fugløybanken (Lindberg and Mienert, 2005) and the mid-Norwegian margin (Svensen et al., 2003; Hovland et al., 2005), co-occurring with pockmarks. This suggests that the living coral reefs may be feeding directly, or indirectly through the water column, from the seepage of hydrocarbon fluids (Hovland and Risk, 2003), although many studies argue against the linkage between fluid seepage and coral reefs (Roberts et al., 2006; Freiwald et al., 1999). Hence we assume that pockmarks are an indicator of mature source rocks below, but are not compulsory since they also need a recording medium (soft sediment) for their formation. As described earlier for the mid-Norwegian margin (Buenz et al., 2005), pockmarks can also form where the gas hydrate stability zone is close to the seafloor. In our study area, the water depths range from 180 to 450 m, hence the stability of gas hydrates varies across the area (Chand et al., 2008). The deepest

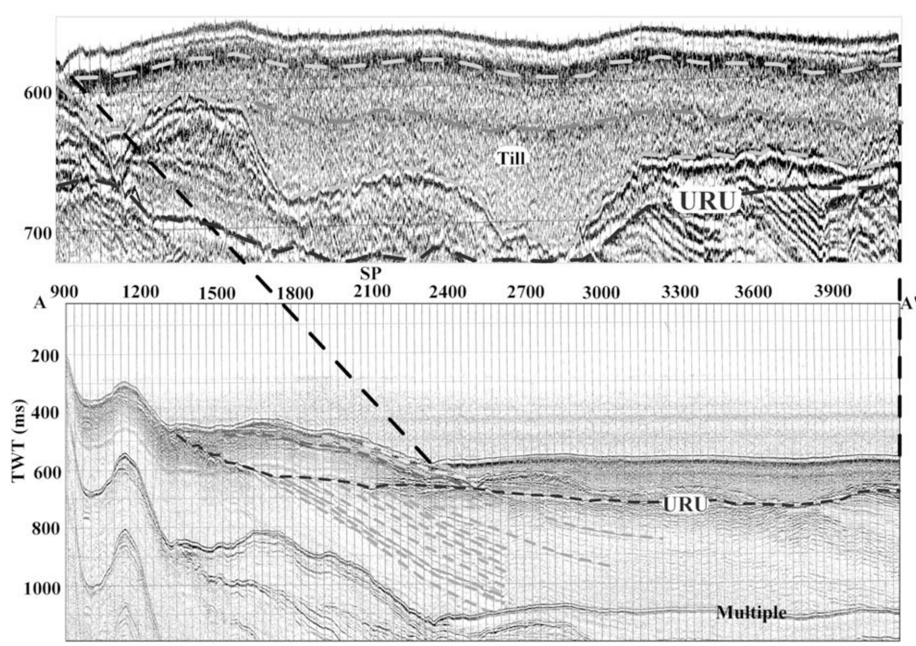

Fig. 8. Near trace plot of a 2D seismic section towards north in Ingøydjupet showing the Quaternary sediments above the upper regional unconformity (URU) where subcropping Mesozoic rocks are truncated by glacial erosion. Pockmarks are found in the upper layer of soft post-glacial clay (location shown in Fig. 1). Line A–A′ shows the angular unconformity formed by glacial erosion of sedimentary and crystalline bedrock.

Please cite this article in press as: Chand, S., et al., Pockmark-like depressions near the Goliat hydrocarbon field, Barents Sea: Morphology and genesis, Marine and Petroleum Geology (2008), doi:10.1016/j.marpetgeo.2008.09.002

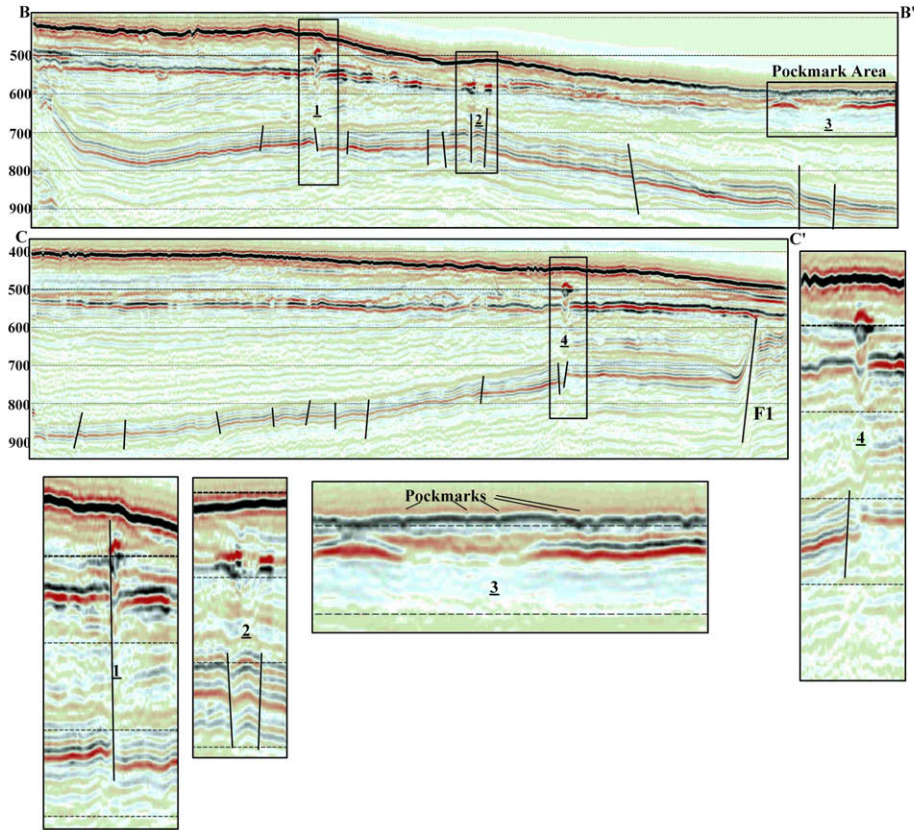

Fig. 9. Seismic lines B–B′ and C–C′ from 3D seismic data (location shown in Fig. 7) across the enhanced reflection area and pockmarks. The left side of the section B–B′ is devoid of pockmarks even though clear indication of gas can be seen. The enhanced reflections are associated with faults connected to deeper layers (see subset Figs. 1, 2 and 5). The pockmark region along the right side of seismic section B–B′ (subset Fig. 5) is without enhanced reflections. The vertical throw of fault F1, running in the NNE–SSW direction (Fig. 7), can be seen in line C–C′.

part of the basin is well into the GHSZ for structure II hydrates (hydrates containing higher order hydrocarbon gases other than methane; Sloan, 1990), with thicknesses of up to 300 m, if 4% of higher order hydrocarbon gases are present along with methane (Chand et al., 2008). GHSZ thickness estimated from the observed BSR depths in the Barents Sea indicates presence of about 4% higher order hydrocarbon gases along with methane (Laberg et al., 1998). Hence, there is likely chance of gas hydrate formation in our study area also although no clear indication of BSR is noticed.

The location of fault F1 close to the pockmark region, and its extension to the no-pockmark region, indicates the importance of the recording medium for the formation of pockmarks. Fault F1 acts as a focussed conduit for fluid flow to the base of the Quaternary sedimentary basin. Diffused flow through the loose sediments thereafter results in an even distribution of pockmarks within individual basins. The absence of pockmarks in the muddy region close to fault F2 indicates the need for fluid source and an open pathway through the fault for the formation of pockmarks. Hence, the recording medium is the most important factor for the formation of pockmarks if gas migrates along well-defined fluid pathways. Gas hydrates can block pockmark formation only in regions of large GHSZ thicknesses, where the stability field cannot be altered by upwelling fluids through small-scale variation of geothermal gradient or through hydrate stability inhibitants such as salt and CO_2.

6. Conclusions

Analysis of high-resolution multibeam bathymetry, 2D/3D seismic data and gas hydrate stability modelling from Tromsøflaket and Ingøydjupet, southern Barents Sea, gives the following conclusions.

1. An area with very high pockmarks intensity has been mapped in a hydrocarbon province in southern Barents Sea. The pockmarks indicate active gas migration and leakage of hydrocarbons to the surface.
2. Pockmarks mainly occur in areas of fine-grained seabed sediments in Ingøydjupet. The intensity of their occurrence, size and depth depend on the soft sediment thickness.
3. Pockmark centres are characterized by increased multibeam backscatter values due to relatively coarse-grained sediments, while pockmark rims are characterized by increased seismic reflection amplitudes possibly due to carbonate cementation.
4. Presence of faults and its coexistence with gas patches indicate an active fluid seepage system although no increase in concentration of pockmarks is associated with it. The diffusive nature of soft sediments overlying the open faults may articulate their formation in a wider region compared to the fault location.

Acknowledgements

We acknowledge the participants of the MAREANO programme (Bathymetric data from the Norwegian Hydrographic Service. Permit No 609/08). We also thank Snorre Olaussen, Johan Leutscher and Stephen Tarran at Eni Norge for useful discussions during the preparation of the manuscript. We thank PL229 operator Eni Norge and partners Statoil and DNO for providing the 3D seismic data. IKU-SINTEF is acknowledged for supplying the 2D seismic data. S. Chand acknowledge GANS project (NFR No. 175969/S30) for funding.

Please cite this article in press as: Chand, S., et al., Pockmark-like depressions near the Goliat hydrocarbon field, Barents Sea: Morphology and genesis, Marine and Petroleum Geology (2008), doi:10.1016/j.marpetgeo.2008.09.002

References

Abrams, M.A., 2005. Significance of hydrocarbon seepage relative to petroleum generation and entrapment. Marine and Petroleum Geology 22, 457–477.

Andreassen, K., Hogstad, K., Bertussen, K., 1990. Gas hydrate in the southern Barents Sea indicated by a shallow seismic anomaly. First Break 8, 235–245.

Bellec, V., Wilson, M., Bøe, R., Rise, L., Thorsnes, T., Mortensen, L.B., Mortensen, P.B., 2008. Bottom currents interpreted from iceberg ploughmarks revealed by multibeam data at Tromsøflaket, Barents Sea. Marine Geology 249, 257–270, doi:10.1016/j.Margeo.2007.11.009.

Bellefleur, G., Riedel, M., Brent, T., 2006. Seismic characterization and continuity analysis of gas hydrate horizons near mallik research wells, Mackenzie Delta, Canada. The Leading Edge, 599–604.

Bass, D.W., Woodworth-Lynas, C., 1988. Iceberg crater marks on the sea floor, Labrador Shelf. Marine Geology 79, 243–260.

Boetius, A., Ravenschlag, K., Schubert, C.J., Rickert, D., Widdel, F., Ieske, A., Amann, R., Jørgensen, B.B., Witte, U., Pfannkuche, O., 2000. A marine microbial consortium apparently mediating anaerobic oxidation of methane. Nature 407, 623–625.

Buenz, S., Mienert, J., 2004. Acoustic imaging of gas hydrate and free gas at the Storegga Slide. Journal of Geophysical Research 109, B04102, doi:10.1029/2003JB002863.

Buenz, S., Mienert, J., Bryn, P., Berg, K., 2005. Fluid flow impact on slope failure from 3D seismic data: a case study in the Storegga Slide. Basin Research 17, 109–122.

Bøe, R., Rise, L., Ottesen, D., 1998. Elongate depressions on the southern slope of the Norwegian Trench (Skagerrak): morphology and evolution. Marine Geology 146, 191–203.

Chand, S., Minshull, T.A., 2004. The effect of hydrate content on seismic attenuation: a case study for Mallik 2L-38 well data, Mackenzie Delta, Canada. Geophysical Research Letters 31, L14609, doi:10.1029/2004GL020292.

Chand, S., Mienert, J., Andreassen, K., Knies, J., Plassen, L., Fotland, B., 2008. Gas hydrate stability zone modelling in areas of salt tectonics and pockmarks of the Barents Sea suggests an active hydrocarbon venting system. Marine and Petroleum Geology 25, 625–636.

Eden, D.J., Eyles, N., 2001. Description and numerical model of Pleistocene iceberg scours and ice-keel turbated facies at Toronto, Canada. Sedimentology 48, 1079–1102.

Farin, N.G.T., 1980. The use of regional geological surveys in the North Sea and adjacent areas in the recognition of offshore hazards. In: Ardus, D.A. (Ed.), Offshore Site Investigation. Graham & Trottman Publishers, London, pp. 5–22.

Freiwald, A., Wilson, J.B., Henrich, R., 1999. Grounding Pleistocene icebergs shape recent deep-water coral reefs. Sedimentary Geology 125, 1–8.

Ginsburg, G.D., Milkov, A.V., Soloviev, V.A., Egorov, A.V., Cherkashev, G.A., Vogt, P.R., Crane, K., Lorensen, T.D., Khutorskoy, M.D., 1999. Gas hydrate accumulation at the Håkon Mosby Mud Volcano. Geo Marine Letters, 57–67.

Guerin, G., Goldberg, D., 2002. Sonic waveform attenuation in gas hydrate bearing sediments from the Mallik 2L-38 research well, Mackenzie Delta, Canada. Journal of Geophysical Research 107 (B5), doi:10.1029/2001JB000556.

Hardage, B.A., Murray, P., Sava, D., Backus, M.M., Remington, R., Graebner, R., Roberts, H.H., 2006. Evaluation of deep water gas hydrate systems. The Leading Edge, 572–576.

Hjelstuen, B.O., Sejrup, H.P., Haflidason, H., Berg, K., Bryn, P., 2004. Neogene and Quaternary depositional environments on the Norwegian continental margin, 62°N–68°N. Marine Geology 213, 257–276.

Hovland, M., 1981. Characteristics of pockmarks in the Norwegian Trench. Marine Geology 39, 103–117.

Hovland, M., 1983. Elongated depressions associated with pockmarks in the western slope of the Norwegian Trench. Marine Geology 51, 35–46.

Hovland, M., Judd, A.G., 1988. Seabed Pockmarks and Seepages. Graham & Trotman, London, 293 pp.

Hovland, M., Risk, M., 2003. Do Norwegian deep-water coral reefs rely on seeping fluids? Marine Geology 198, 83–96.

Hovland, M., Svensen, H., Forsberg, C.F., Johansen, H., Fichler, C., Fosså, J.H., Jonsson, R., Rueslåtten, H., 2005. Complex pockmarks with carbonate ridges off mid Norway: products of sediment degassing. Marine Geology 218, 191–206.

Hubscher, C., Borowski, C., 2006. Seismic evidence for fluid escape from Mesozoic cuesta type topography in the Skagerrak. Marine and Petroleum Geology 23, 17–28.

King, L.H., 1980. Aspects of regional surficial geology related to site investigations requirements – Eastern Canadian Shelf. In: Ardus, D.A. (Ed.), Offshore Site Investigation. Graham & Trottman Publishers, London.

King, L.H., MacLean, B., 1970. Pockmarks on the Scotian Shelf. Geological Society of America Bulletin 81, 3141–3148.

Laberg, J.S., Andreassen, K., Knutsen, S.M., 1998. Inferred gas hydrate on the Barents Sea Shelf a model for its formation and a volume estimate. Geo Marine Letters 18, 26–33.

Lindberg, B., Mienert, J., 2005. Postglacial carbonate production by cold water corals on the Norwegian Shelf and their role in the global carbonate budget. Geology 33, 537–540.

Macdonald, I.R., Sager, W.W., Peccini, M.B., 2003. Gas hydrate and chemosynthetic biota in mounded bathymetry at mid-slope hydrocarbon seeps: Northern Gulf of Mexico. Marine Geology 198, 133–158.

Maisey, G.H., Rooengen, K., Raaen, K., 1980. Pockmarks Formed by Seep of Petrogenic Gas in the Southern Part of the Norwegian Trench. Continental Shelf Institute, Norway. Rep P-258.

McQuillin, R., Farin, N.G.T., Judd, A., 1979. IS Pockmark Investigations 1974–1978. Institute of Geological Sciences, Continental Shelf Division, Marine Geophysics Unit, Report 98, 50 pp.

Mienert, J., Posewang, J., Baumann, M., 1998. Gas hydrates along the northeastern Atlantic margin: possible hydrate-bound margin instabilities and possible release of methane. In: Henriet, J.P., Mienert, J. (Eds.), Gas Hydrates: Relevance to World Margin Stability and Climate Change. Geological Society, London, Special Publication, vol. 137, pp. 275–291.

Nouze, H., Henry, P., Noble, M., Martin, V., Pascal, G., 2004. Large gas hydrate accumulations on the eastern Nankai Trough inferred from new high resolution 2-D seismic data. Geophysical Research Letters 31, L13308, doi:10.1029/2004GL019848.

Paull, C., Ussler III, W., Maher, N., Greene, H.G., Rehder, G., Lorenson, T., Lee, H., 2002. Pockmarks off Big Sur, California. Marine Geology 181, 323–335.

Ritger, S., Carson, B., Suess, E., 1987. Methane derived authigenic carbonates formed by subduction induced pore water expulsion along the Oregon/Washington margin. Geological Society of America Bulletin 98, 147–156.

Rise, L., Sættem, J., Fanavoll, S., Thorsnes, T., Ottesen, D., Bøe, R., 1999. Sea bed pockmarks related to fluid migration from Mesozoic bedrock strata in the Skagerrak offshore Norway. Marine and Petroleum Geology 16, 619–631.

Rise, L., Rokoengen, K., Skinner, A.C., Long, D., 1984. Northern North Sea Quaternary Geology Map Between 60° 30′ and 62°N and East 1°E, 1:50 000. Institut for Kontinentalsokkel Undersøkelser (IKU), Trondheim, Norway.

Roberts, J.M., Wheeler, A.J., Freiwald, A., 2006. Reefs of the deep: the biology and geology of cold-water coral ecosystems. Science 312, 543–547.

Sassen, R., Losh, S.L., Cathles III, L., Roberts, H.H., Whelan, J.K., Milkov, A.V., Sweet, S.T., DeFreitas, D.A., 2001. Massive vein filling gas hydrate: relation to ongoing gas migration from the deep subsurface in the Gulf of Mexico. Marine and Petroleum Geology 18, 551–560.

Sloan, E.D., 1990. Clathrate Hydrates of Natural Gases. Marcel Dekker, New York.

Solheim, A., Elverhøi, A., 1985. A pockmark field in the central Barents Sea; gas from a petrogenic source. Polar Research 3, 11–19.

Svensen, H., Planke, S., Jamtveit, B., Pedersen, T., 2003. Seep carbonate formation controlled by hydrothermal vent complexes a case study from the Vøring Basin, the Norwegian Sea. Geo Marine Letters 23, 351–358.

Svitzer, 2001. Regional Site Survey, PL229, vol. 1: Text 621 and Track Charts. Final Report 622, Norsk Agip A/S, Project: 23-940, 127 pp.

Todd, B.J., Fader, G.B.J., Courtney, R.C., Pickrill, R.A., 1999. Quaternary geology and surficial sediment processes, Browns Bank, Scotian Shelf, based on multibeam bathymetry. Marine Geology 162, 165–214.

Van Rensbergen, P., Rabaute, A., Colpaert, A., St. Ghislain, T., Mathijis, M., Bruggeman, A., 2007. Fluid migration and fluid seepage in the Connemara Field, Procupine Basin interpreted from industrial 3D seismic and well data combined with high-resolution site survey data. International Journal of Earth Sciences 96, 185–197.

Van Weering, T., 1982. Shallow seismic and acoustic reflection profiles from the Skagerrak; implications for recent sedimentation. Proceedings of the Koninklijke Nederlandse Academie van Wetschappen, B 85, 129–154. Amsterdam.

Van Weering, T., Jansen, J.H.F., Elisma, D., 1973. Acoustic reflection profiles of the Norwegian Channel between Oslo and Bergen, Netherlands. Journal of Sea Research 6, 241–263.

Vorren, T.O., Richardsen, G., Knutsen, S.M., Henriksen, E., 1991. Cenozoic erosion and sedimentation in the western Barents Sea. Marine and Petroleum Geology 8, 317–340.

Whiticar, M.J., Werner, F., 1981. Submarine vent of natural gas to freshwater seeps? Geo Marine Letters 1, 193–199.

Widess, M.B., 1973. How thin is a thin bed? Geophysics 38, 1176–1180.

WOD05, 2005. World Ocean Database Available from: http://www.nodc.noaa.gov/General/temperature.html.

Please cite this article in press as: Chand, S., et al., Pockmark-like depressions near the Goliat hydrocarbon field, Barents Sea: Morphology and genesis, Marine and Petroleum Geology (2008), doi:10.1016/j.marpetgeo.2008.09.002